Military Technical College
Kobry El-Kobbah,
Cairo, Egypt

6th International Conference
on Electrical Engineering
ICEENG 2008

Computer simulation of the sky wave propagation through the disturbed ionosphere

By

Mohamed A H Eleiwa

Abstract
A computer model is presented for the performance assessment of HF ionospheric communication links. The proposed model considers the effects of the natural and artificial ionospheric disturbances on the radio waves propagation parameters and modes. The ionosphere and radio wave parameters are first derived for specified ionospheric communication links. The natural and/or artificial disturbances are assumed over the link path, and the resulting modified propagation medium and wave parameters are then estimated and compared with their corresponding parameters for quiet ionosphere. Hence, the link performance is evaluated and guide lines for retuning the communication link are proposed to control (enhance or disrupt) the ionospheric communication links. The ionosphere and wave parameters are derived for different communication links subjected to natural disturbances due to different solar activities, solar flares, and geomagnetic storms. Several communication links are also analyzed under the effect of artificial modification by HF ionospheric heaters.

Keywords: Radio wave propagation, Ionospheric communication links, Natural and artificial ionosphere modification

---

* Egyptian Armed Forces

I. Introduction

Although nowadays most long distance radio communications are done with the use of satellites, ionospheric (sky) radio wave still provides an efficient and cost effective means of radio communication [1-2]. It also still plays an important role in the study of the structure of the ionosphere [3]. The ionosphere is the region from about 60 km to 2000 km altitude, where the solar irradiance produces partially ionized plasma of mostly H^+ and He^+ above 1000 km, O^+ from 300 to 500 km and molecular ion (NO^+, O_2^+, N_2^+) below 200 km. An HF wave is not simply reflected once at a single critical altitude, it is continuously refracted as it traverses the ionosphere, and long-distance communications is the result of refraction. Depending on the frequency used and the time of day, the ionosphere can support communications from very short ranges of less than 90 km (called near vertical incidence sky wave; NVIS) to distances of greater than 4000 km on a single hop and up to global distances with multi-hop propagation.

For successful radio communication, it is essential to predict the behavior of the ionosphere region that will affect a certain radio communication link. Such a prediction will identify the time periods, the path regions, the frequency, and the transmitted power, the receiver sensitivity, transmitting and receiving antennas parameters. Accurate prediction for the performance of the ionospheric communication links requires accurate modeling of the ionosphere. Several physical, empirical, and semiempirical models [4-8] have been developed to predict ionospheric variables. Measurements of the critical frequencies of the ionospheric regions (f_oE, f_oF1, and f_oF2) obtained at South America stations for different solar conditions and seasons were used in [9-10] to check the validity of the international reference ionosphere (IRI) model. Several computer programs have been developed for the analysis of ionospheric communication links such as ICEPAC [11], IONCAP [12], VOACAP [13], and their parent model, ITSA [14]. A review and comparison study for some of these models is presented in [15]. All these models consider only the effects of solar activity on some of the sky wave propagation parameters [16-20].

Because HF communications are controlled directly by the ionosphere's properties, an artificially created ionization region with tailored characteristics could be used to enhance or disrupt radio waves propagation over specific ionospheric communication links. The artificial ionospheric modification has been proven experimentally using HF heating facilities [21-25]. High-frequency modification produces large scale ionospheric variations and parametric instability which alter HF propagation characteristics. Understanding how to control the spectrum of the artificial irregularities generated by the HF ionosphere heaters should be a primary goal of research in this area. Additionally, it may be possible to control the growth of natural irregularities resulting from natural environmental effects. Therefore, this paper presents a simplified and comprehensive model to predict the performance of the ionospheric communication links under the effects of natural and artificial ionospheric disturbances. The parameters of the natural or the artificial ionospheric disturbances are first input to the proposed code. The ionospheric medium and radio wave parameters are then calculated and compared for both undisturbed and disturbed ionosphere over a given HF communication link. Hence, the ionospheric link performance is predicted and analyzed. Guide lines for the communication link retuning are also provided and discussed. A simplified propagation model in the ionosphere is presented in section II. The modified ionospheric parameters due to natural and artificial disturbances are derived in section III, where the effects of solar activities on the radio wave propagation parameters are derived, calculated, discussed, and compared. Also, the effects of some heating experiments on the ionospheric medium and wave parameters are discussed and analyzed, and hence the conditions for the best or the worst ionospheric

propagation modes are illustrated numerically and graphically. Finally, discussions and conclusions are presented in section IV.

II. Modeling electromagnetic waves propagation in the Ionosphere

Assuming a linearly y-polarized electromagnetic wave propagating through an imperfectly conducting medium such as the ionosphere along the z-direction, the instantaneous electric field E_y component of the propagating wave is described as

$$\mathbf{E_y = E_o e}^{\mathbf{j\omega\left(t-\frac{z\sqrt{\varepsilon_c'}}{c}\right)}} \quad (1)$$

Where ε_c' is the relative complex permittivity of the ionosphere. The simplest approach to describe the radio wave propagation through the ionosphere is to solve for the index of refraction. Thus, substituting the following equation

$$\sqrt{\varepsilon_c'} = \sqrt{\left(\frac{\varepsilon}{\varepsilon_o} - \mathbf{j}\frac{\sigma}{\omega\varepsilon_o}\right)} = \sqrt{\varepsilon' - \mathbf{j}\varepsilon''} = \mathbf{n - jp} \quad (2)$$

into equation (1) to yield

$$\mathbf{E_y = E_o e}^{-\frac{\omega}{c}\mathbf{pz}}\mathbf{e}^{\mathbf{j\omega\left(t-\frac{nz}{c}\right)}} \quad (3)$$

Solving equation (2) to give the coefficients n and p as

$$\mathbf{n} = \pm\sqrt{\mathbf{0.5}\left(\varepsilon' + \sqrt{(\varepsilon')^2 + (\mathbf{60}\sigma\lambda)^2}\right)} \quad (4)$$

$$\mathbf{p} = \pm\sqrt{\mathbf{0.5}\left(-\varepsilon' + \sqrt{(\varepsilon')^2 + (\mathbf{60}\sigma\lambda)^2}\right)} \quad (5)$$

The homogeneous ionized gas (ionosphere) behaves like an imperfectly conducting medium with conductivity σ_i and dielectric constant ε_i' which are given by [10] as

$$\varepsilon_i' = \mathbf{1} - \frac{\omega_p^2}{\omega^2 + \nu^2} \quad (6)$$

$$\sigma_i = \frac{\varepsilon_o\omega_p^2\nu}{\omega^2 + \nu^2} \quad (7)$$

Where $\omega = \mathbf{2\pi f}$ is the propagating wave frequency, v is the collision frequency, $\omega_p = \sqrt{\frac{N_e q_e^2}{m_e\varepsilon_o}} = \mathbf{2\pi f_p}$ is the plasma frequency, N_e is the density of free electrons, m_e, and q_e are mass and charge of the electron. Alternatively, from statistical mechanics, the electrical conductivity of a free electron gas can be calculated as $\sigma_i = \mathbf{N_e q_e^2 \tau / m_e}$, where $\tau = \mathbf{l_{mfp}}\left(\mathbf{m}/\mathbf{3K_BT}\right)^{0.5}$ is the average time

between electron collisions, l_{mfp} is the mean free path between electron collisions, $\mathbf{K_B}$ is Boltzman constant, and T is the absolute temperature in Kelvin. It is clear from equation (3) that as the radio waves travel through an imperfectly conducting medium, such as the ionosphere, short waves experience phase change with coefficient $\beta = \frac{\mathbf{n}\omega}{\mathbf{c}}$. The phase velocity is given by $\mathbf{v_p = c/n}$, while the corresponding group velocity is $\mathbf{v_g = nc}$, where c is the light speed and n is the refractive index of equation (4). Also, the propagating waves experience attenuation due to the absorption of energy. The extent of attenuation is characterized by the absorption coefficient $\alpha = \frac{\mathbf{p}\omega}{\mathbf{c}}$, and p is as given by equation (5). In the presence of terrestrial magnetic field ($\mathbf{B_o = \mu_o H_o}$), the electron rotates and exhibits resonance characteristics called gyro magnetic resonance with gyro frequency $\mathbf{f_m = q_e \mu_o H_o /(2\pi m_e)}$, $\omega_m = 2\pi f_m$. Also, the conductivity in magnetized plasma is represented in a tensor form with elements: Pederson $\sigma_P = \frac{\nu^2}{\omega_m^2 + \nu^2}\sigma_O$, Hall $\sigma_H = \frac{\omega_m \nu}{\omega_m^2 + \nu^2}\sigma_O$, and the parallel conductivity $\sigma_{\parallel} = \sigma_O = \frac{N_e q_e^2}{m_e \nu} = \sigma_i(\omega = 0)$. Substituting equations (6) and (7) into equation (4) to give another alternative form of refractive index of the ionosphere as

$$\mathbf{n^2 = 1 - \frac{\omega_p^2}{\omega(\omega + j\nu)}} \qquad (8)$$

The presence of the earth's magnetic field makes the ionosphere a double refractive medium. Using the Appleton-Hartree dispersion relation [1], the refractive index n, is generally given by

$$\mathbf{n_{O,X}^2 = 1 - \frac{X}{1 - jZ - \frac{Y_T^2}{2(1 - X - jZ)} \pm \left(\frac{Y_T^4}{4(1 - X - jZ)^2} + Y_L^2 \right)^{0.5}}} \qquad (9)$$

For HF waves (***f = 3: 30 MHz***), where $\nu << \omega$, then $Z = \nu/\omega$ ***~0***, the refractive index n is simplified as

$$\mathbf{n_{O,X}^2 = 1 - \frac{X(1 - X)}{(1 - X) - 0.5Y_T^2 \pm \left(0.25Y_T^4 + (1 - X)^2 Y_L^2\right)^{0.5}}} \qquad (10)$$

Where $\mathbf{X = \omega_p^2/\omega^2}$, $\mathbf{Y = \omega_m/\omega}$, $\mathbf{Y_L = Y\cos\phi}$, $\mathbf{Y_T = Y\sin\phi}$ and ϕ is the angle between the direction of propagation and the geomagnetic field. The '+' sign refers to the ordinary (***O***-mode) wave and the '-'sign refers to the extraordinary (***X***-mode) wave.

Actually, the refractive index of the ionosphere is not constant but it is a function of the ray path. Assuming the refractive index ***n(z)*** is a slowly varying function of height z above the surface of the earth. Suppose that an up going radio wave of amplitude E_o is generated on the ground level (***z=0***). The complex amplitudes of the wave are given by the approximate solutions of the non-uniform wave equation, which are commonly called the W.K.B. (Wentzel, Kramers, and Brillouin) solutions [26], and are given by

$$\mathbf{E_y \approx E_o n^{-0.5} exp\left(\pm jk \int_0^z n(z) dz \right)} \quad (11)$$

$$\mathbf{cB_x \approx «E_o n^{0.5} exp\left(\pm jk \int_0^z n(z) dz \right)} \quad (12)$$

Assuming that the wave is reflected at the plane $z=z_o$ where $\omega = \omega_p(z_o)$, with reflection coefficient ***R,*** which is given by

$$\mathbf{R = -j exp\left(2jk \int_0^{z_o} n(z) dz \right)} \quad (13)$$

For an obliquely incident wave on the ionosphere with incidence angle ψ_i as shown in Fig.1, the W.K.B. solutions are simply obtained by replacing the refractive index ***n*** in equations (11), (12), and (13) by the parameter ***q***, where $q^2 = n^2 - \sin^2 \psi_i$, and the ray tracing equation in the ***x-z*** plane is given by

$$\mathbf{x = \sin \psi_i \int_0^z \frac{dz}{\sqrt{n^2(z) - \sin^2 \psi_i}}} \quad (14)$$

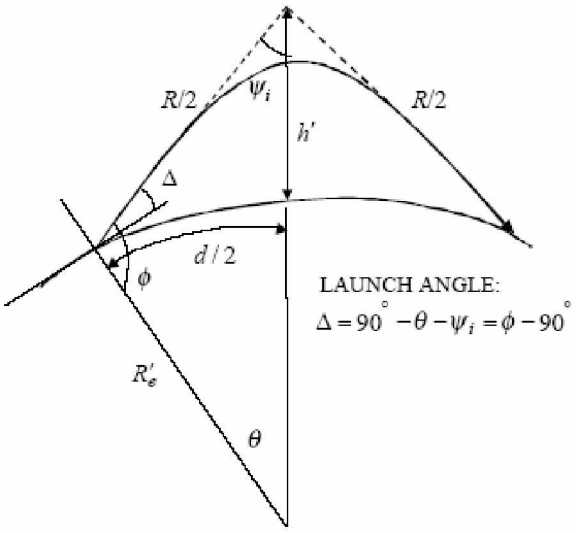

Fig.1 Geometry of incident, reflected, and refracted rays in the ionosphere

From equation (14) and Fig.1, the ray eventually intersects the earth's surface again at a horizontal distance given by

$$\mathbf{x_o = 2 \sin \psi_i \int_0^{z_o(\sin \psi_i)} \frac{dz}{\sqrt{n^2(z) - \sin^2 \psi_i}}} \quad (15)$$

Consider Fig.1, and using the law of sines for a triangle, the relation between the incidence angle (ψ_i) and the launch angle (elevation angle; ***Δ***) is given by

$$\sin\psi_i = \frac{\cos\Delta}{1+h'/R_e} \tag{16}$$

Alternatively, the incidence angle is given by $\tan\psi_i = R_e \sin\theta / \left(h' + R_e(1-\cos\theta)\right)$. The geocentric angle θ in degrees is given by $\theta^o = d/(296.7 \times nh)$ where d is the total length of the ionospheric radio link in *km*, and *nh* is the number of reflections (hops). The maximum angle of incidence ($\psi_{i\,max}$) is obtained when $\Delta=0$ (the incident ray tangent to the earth's surface). Hence, $\sin\psi_{imax} = \frac{1}{1+h'/R_e}$, where h' is the virtual height and R_e*=8500 km* is the effective earth's radius for a curved earth model. A plot of the function $h' = F(f)$ is called an ionogram or a height-vs.-frequency characteristic. For the ray to return to the earth, the angle of incidence at the n^{th} ionosphere stratum may approach 90^o. Thus, the relation between the electron density N_n and the corresponding frequency f at certain height h may be derived by substituting equations (8) and (16) into Snell's law of refraction to give

$$f = \frac{1}{2\pi}\sqrt{\left(\frac{3190\,N_n\left(1+\frac{2h'}{R_e}\right)}{\sin^2\Delta + \left(\frac{2h'}{R_e}\right)}\right) - \nu^2} \tag{17}$$

From equation (17), the maximum usable frequency MUF is obtained at zero elevation angles and at maximum electron density. For HF waves, where $\nu << \omega$, the collision frequency may be neglected, and the maximum usable frequency is approximately given by the maximum value of equation (17) as $MUF \approx 8.984\sqrt{N_{max}}$. Under the effect of the longitudinal B_o ($B_L = B_o \cos\phi$), the maximum usable frequency (neglecting collision frequency) can be derived by substituting $Y_T=0$ and the condition of reflection into equation (10) to give $MUF \approx 8.984\sqrt{N_{max}} \ll f_m \cos\phi$ for vertically incident (*O*-mode) and (*X*-mode); respectively. Similarly, the maximum usable frequencies can be derived in the presence of the transverse component of terrestrial magnetic flux density B_o ($B_T = B_o \sin\phi$).

Starting from the attractive Coulomb force exerted by an ion on an electron, the electron-ion collision frequency ν_{ei} is given by

$$\nu_{ei} = \frac{\omega_p^4\sqrt{2}}{64\pi N_e}\left(\frac{K_B T_e}{m_e}\right)^{-3/2} \tag{18}$$

Where K_B = *1.38x10*$^{-23}$ *Joule / °C* is Boltzman constant. Generally, the collision frequency ν is given by [26] as

$$\nu = 3.3\times10^{-16}\sqrt{T}\left[N(O_2) + N(N_2) + 2N(O)\right] \tag{19}$$

Where ***N (O2), N (N2)*** and ***N (O)*** are the densities in ***[m^{-3}]*** of ***O2***, ***N2*** and ***O*** in the atmosphere. The temperature ***T*** is in Kelvin. The particles collisions absorb energy from the propagating radio wave. This form of absorption is known as non-deviative (ε_i' is constant) absorption (α_{nd}), which can be derived from the general expression of the absorption coefficient $\alpha = \frac{p\omega}{c}$ for HF wave propagating in the (quiet) ionosphere, where the displacement current is usually much greater than the convection current. Then, after simple mathematical manipulation, one can get

$$\alpha_{nd} = 1.35 \times 10^{-7} \frac{N\nu}{f^2} \qquad (20)$$

III. Modified ionospheric radio communication links

Normally, the ionosphere is not a stable medium that allows the use of the same frequency throughout the year, or even over 24 hours. The ionosphere varies with the time, seasons, latitude, longitude, with solar cycle and its consequences of solar flares and geomagnetic storms. Flares and other energetic events on the Sun produce increased ultraviolet, x-ray and gamma-ray photons that dramatically increase the density of the ionosphere on the dayside after arrival at the Earth. The activity of the ionosphere is strongly affected by the number of the sunspots. The number of sunspots ***(SSN)*** on the sun at any given time varies in an 11-year cycle as does the number and severity of disturbances in space weather [27]. The solar flux ***(SF)*** is another measure of the solar activity, and it is the amount of radio flux emitted at a frequency of 2.8 GHz. The empirical relation between the average solar flux and average sunspot number is derived from measured data and is found to be $SF = 8.9 \times 10^{-4} (SSN)^2 + 0.728 \times SSN + 63.7$, which is plotted in Fig.2. The level of geomagnetic activity is determined by the ***A*** and ***K*** indices. The daily A index has a linear scale from 0 (quiet) to 400 (severe storm), the three-hour K index has a quasi-logarithmic scale from 0 to 9, a compressed version of the A index, with 0 being quiet and 9 being severe storm. These give indications of the severity of the magnetic fluctuations and hence the disturbance to the sky wave communications through the ionosphere. The A-index is plotted vs. K-index in Fig.3, where different geomagnetic activities are defined in terms of the A and K indices.

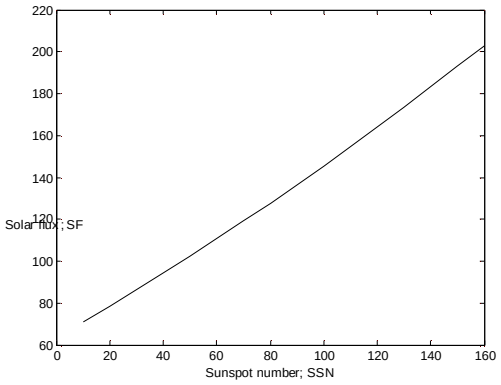

Fig.2 The empirical relation between the sunspot number and solar flux

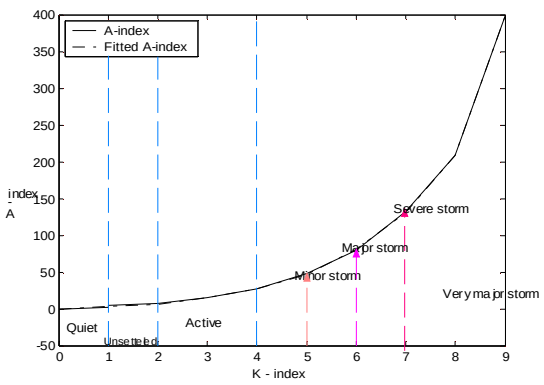

Fig.3 Different geomagnetic activities as described by the A and K indices

The fitting polynomial which describes the relation between the A-index and K-index is derived and found to be

$$\mathbf{A = 0.005K^7 - 0.131K^6 + 1.444K^5 - 7.899K^4 + 22.537K^3 - 30.022K^2 + 17.157K - 0.028}$$

Generally, the critical frequencies of the ionospheric E and F layers are influenced by the solar activities as shown in Fig. 4, where the measured critical frequencies are averaged and plotted vs. the sunspot numbers at different times, seasons and years, and are found to be generally increasing as SSN increases.

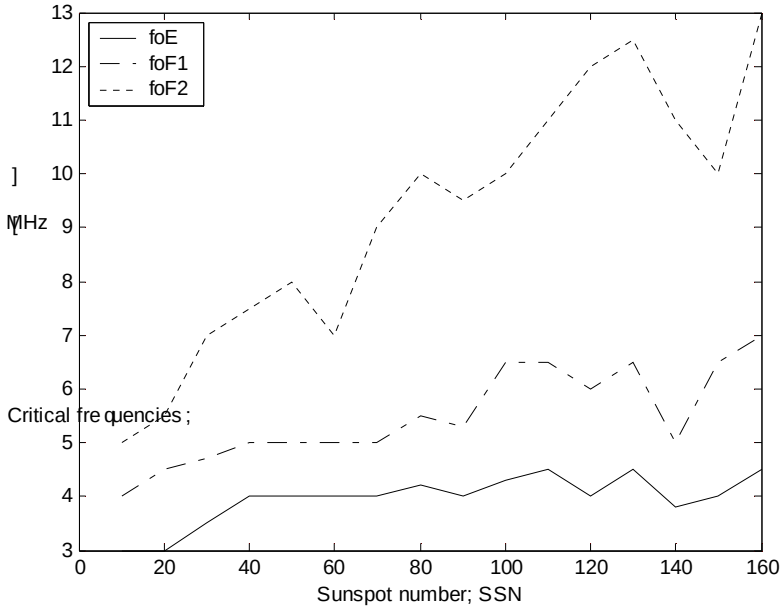

Fig.4 Average measured critical frequencies vs. sunspot number

Further investigation of the effects of natural ionosphere disturbances due to variable solar activities on the sky wave propagation is studied by analyzing a specific ionospheric communication link. The transmitter link station is assumed to be in Alaska; USA (62.39 N, 145.15 W), while the remote receiving station is in Cairo; Egypt (30.03 N, 31.15 E).

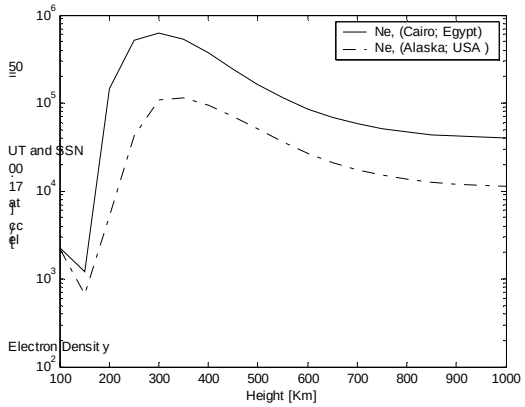

Fig.5 Electron density vs. height above link terminals at SSN = 50, 17.00 UT.

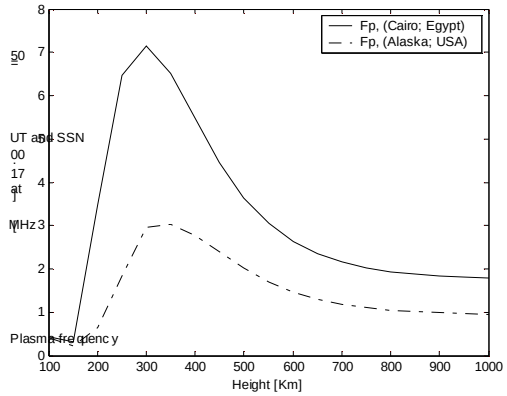

Fig.6 Plasma frequency vs. height above link terminals at SSN = 50, 17.00 UT.

The electron density variations vs. height above the link terminals in Alaska and Cairo are first studied using MSIS model at sunspot number SSN = 50 and universal time UT = 17.00, as shown in Fig.5. Then the corresponding plasma frequency variations are found using the model equations derived in the previous section and shown in Fig.6. The critical frequencies of different ionospheric layers; E, F1 and F2, are also found and their variations vs. SSN are derived, compared and plotted in Fig.7 and Fig.8 at link terminals at different universal times

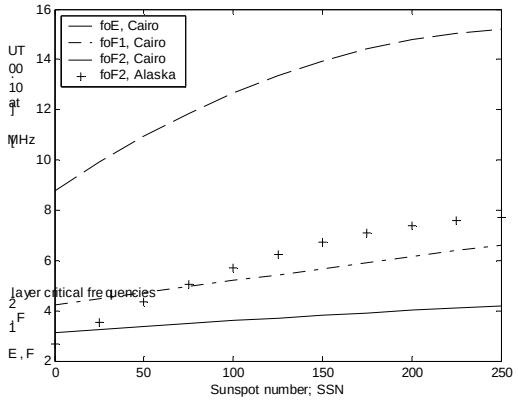

Fig.7 Critical frequency vs. SSN above link terminals at 10.00 UT.

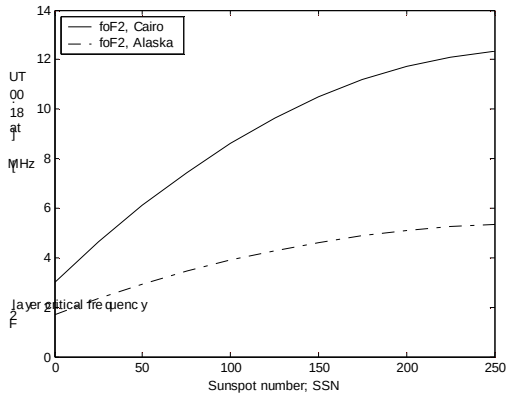

Fig.8 Critical frequency vs. SSN above link terminals at 18.00 UT.

The densities of the constituent particles (oxygen and nitrogen) for the ionosphere region at UT = 15.00 and height h = 100 km above the receiving station in Cairo are plotted vs. SSN in Fig.9, and compared for both quiet (A = 0) and stormy (A = 80) geomagnetic conditions. Also, the neutral (T_n), ion (T_i) and electron (T_e) temperatures are plotted and compared vs. height at SSN = 50 and UT = 17.00 above link terminals in Cairo and Alaska, as shown in Fig.10.

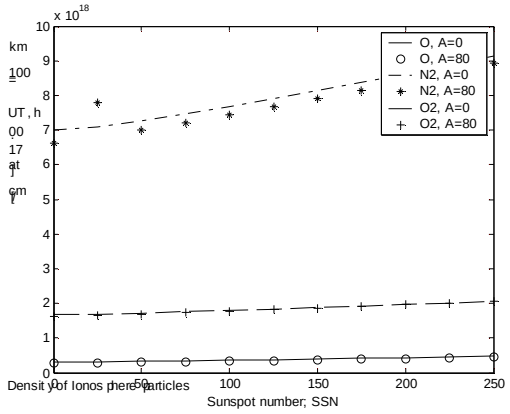

Fig.9 Ionosphere particles densities vs. SSN for quiet and stormy ionosphere above Cairo

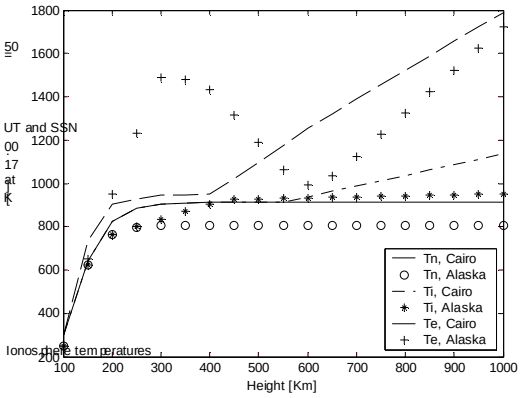

Fig.10 Ionosphere particles temperatures vs. height above link terminals

Substituting the data of Fig.9 and Fig.10 into equation (19) to get the electron collision frequency ν_e. The variation of ν_e vs. SSN at UT = 15.00 and height h = 100km above cairo is plotted in Fig.11 and compared for both quiet and stormy geomagnetic conditions.

.

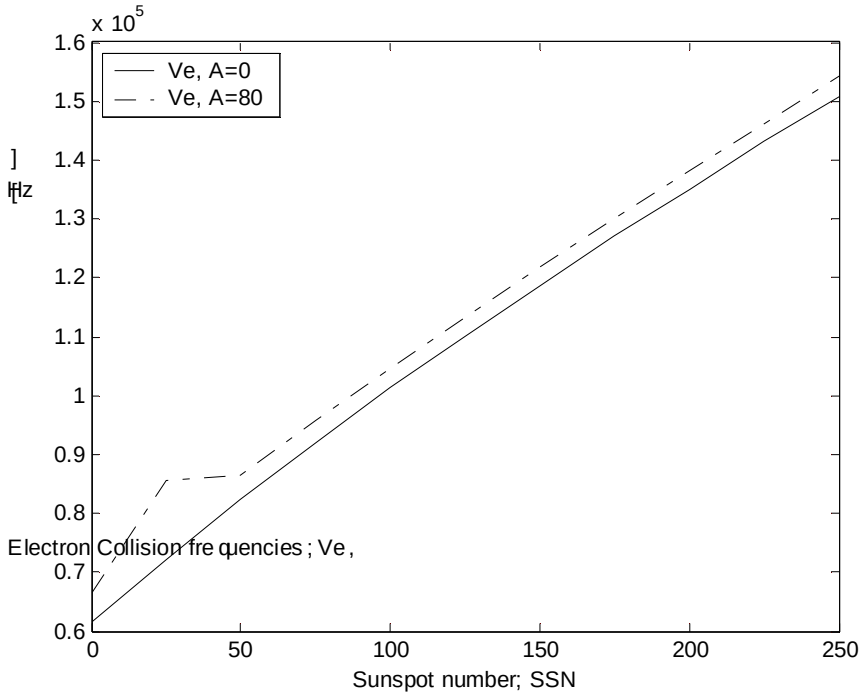

Fig.11 Electron collision frequency vs. SSN for quiet and stormy ionosphere above Cairo

The dielectric constant and conductivity of the ionosphere are then calculated and substituted into equations (4) and (5) to yield n and p, and hence the phase (β) and absorption (α)coefficients are calculated and plotted vs. SSN at different frequencies, as shown in Fig.(12) and Fig.(13).

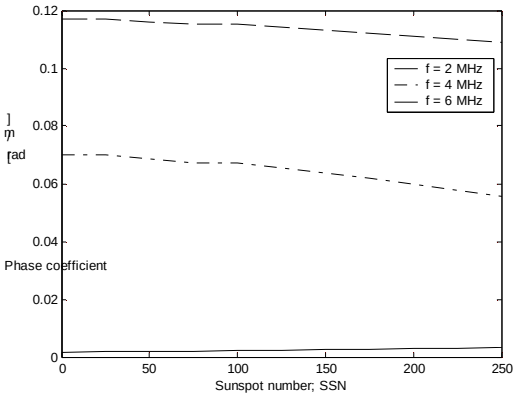

Fig.12 Phase coefficient variation vs. SSN at different frequencies.

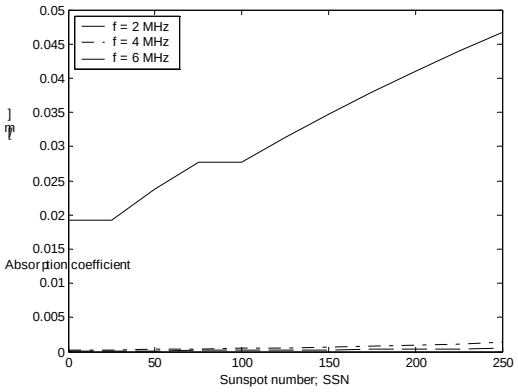

Fig.13 Absorption coefficient variation vs. SSN at different frequencies.

To study the effect of the artificial ionosphere modification using powerful ground-based HF heating facilities, the electron temperature variations (T_e) due to heating of the ionosphere above Alaska by HAARP heating facility using different transmitted HF powers with ERP = 83.4 dB and 95.7 dB are reported by [28] and plotted vs. height in Fig.14 and compared with the corresponding T_e but for unheated ionosphere.

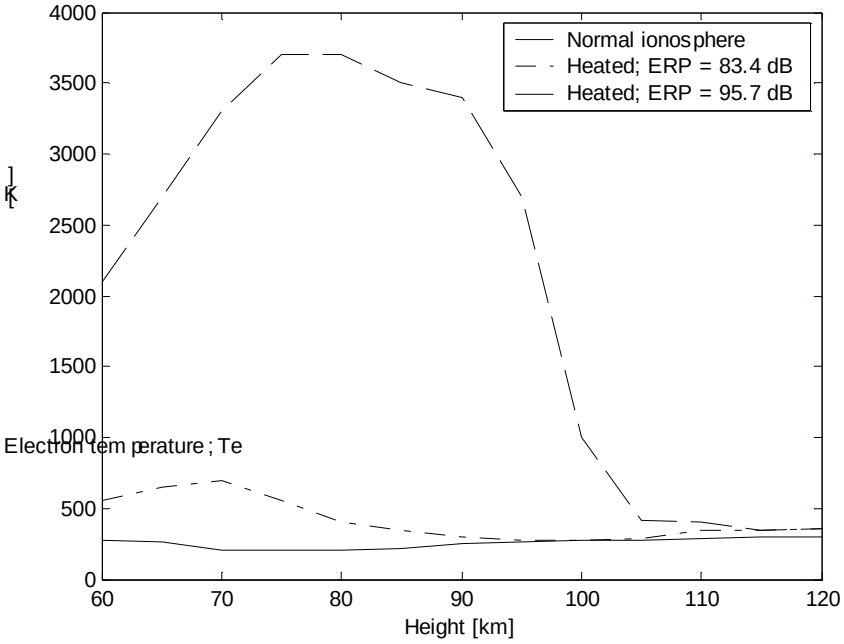

Fig.14 Electron temperatures vs. height for heated and unheated ionosphere above Alaska

Another ionospheric heater example; Sura heating facility (56.15 N, 44.3 E) in Russia, is considered. The heating experiment has been performed by [29] on October 4, 1991 at 16.30 LT. The resulting density profile is compared with that for the unheated (normal) ionosphere and plotted in Fig.15. The consequent variation in plasma frequency is derived and compared with the normal one as shown in Fig.16.

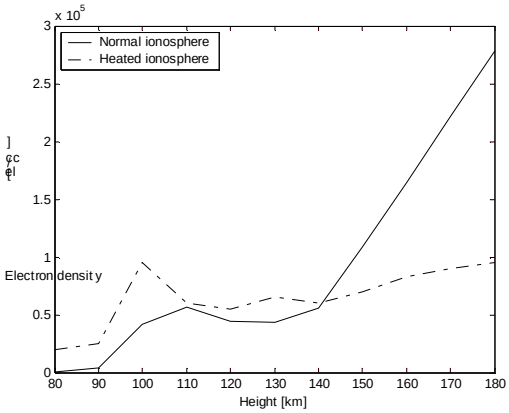

Fig.15 Electron density profiles for normal and heated ionosphere

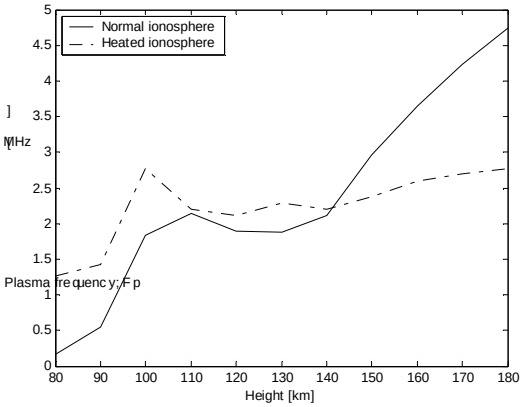

Fig.16 Plasma frequency vs. height for normal and heated ionosphere

IV. Discussions and conclusions

Knowledge of the ionospheric electron density is essential for radio and telecommunications applications. The ionosphere is usually described by an electron density profile as a function of height. The ionosphere electron density profile varies also with latitude, longitude, and time, solar flares and geomagnetic storms along the propagation path. Therefore in the proposed model, the electron density profiles have been firstly derived for the modified ionosphere and compared with those for the undisturbed ionosphere. The ionosphere medium and HF propagating wave parameters have then been derived, calculated and compared. Also, different empirical relations have been derived to describe the relations among solar and geomagnetic activities parameters, as shown in figures 2, 3, and 4. The impact of the natural and artificial ionospheric modifications on the performance of ionospheric communication links have been investigated by considering an example of an ionospheric communication link between Alaska in USA and Cairo in Egypt. The numerical results showed clearly the dependence of electron density, and consequently plasma and critical frequencies on solar activity parameter (SSN), time and position as shown in figures 5, 6, 7, and 8. From the obtained numerical results, it is essential to have an MUF daily schedule at each remote station to state the recommended MUF at each hour depending on solar and geomagnetic activities. The electron collision frequency have been found comparable to plasma frequency, especially at lower ionospheric D and E regions as shown in Fig.11, where $\boldsymbol{\nu_e}$ varies with solar and geomagnetic activity parameters; SSN and A respectively. The obtained $\boldsymbol{\nu_e}$ values comparable to plasma frequency recommend equation (17) as an accurate relation between HF frequency f and Electron density N_e. The variation of phase and absorption coefficients vs. the sun spot number has also been investigated and plotted in figures 12 and 13, where higher frequencies suffer from higher phase change and absorption, especially in the lower D and E ionosphere regions. The artificial ionospheric modification has been investigated by using different HF heating facilities; HAARP in Alaska (USA) and Sura in Russia. Fig.14 shows clearly the severe ionosphere disruption by increasing the electron temperature T_e up to 3500 K due to HAARP heater power with ERP = 95.7 dB compared to 300 K for unheated ionosphere. Consequently, the electron density in the E region increases as a result of active heating because of the recombination rate reduction; $\alpha_{rc} \propto \left(1/T_e^{0.8}\right)$. On the other hand, the electron collision frequency $\boldsymbol{\nu_e}$ increases. Both factors strongly recommend E blanketing mode due to reflection from the strongly ionized E layer and / or increased absorption due to in creased $\boldsymbol{\nu_e}$ according to equation (20). Also, the sura heating facility strongly modifies the electron density profile during heating experiment as shown in figures 15 and 16, where the electron density and the plasma frequency have been increased at lower heights up to 140 km. In conclusion, disruption of HF communications due to ionosphere disturbances can be avoided by increasing transmitted power and using better antennas. Progressively decreasing or increasing frequencies after the onset of an ionosphere disturbance to counteract the resulting decrease or increase in the ionosphere electron density, and finally HF rely stations to be designed and located outside the disturbance area.

References

[1] K. Davies, "Ionospheric Radio," Peter Peregrinus Ltd., London, 1990.
[2] K. G. Budden, 'Radio waves in the ionosphere," Cambridge Univ. Press, New York, 1961.
[3] Hunsucker, R.D., "Radio Techniques for Probing the Terrestrial Ionosphere," Springer-Verlag:Berlin, 1991.
[4] D. N. Anderson, and B. Hertniter, "A semiempirical low altitude ionospheric model," Radio Sci., 22, 292, 1987.
[5] D. Bilitza, "International Reference Ionosphere: Recent developments," Radio Sci., 21, 343, 1986.

[6] B. A. Hausman, New Ionospheric and Magnetospheric Specification Models, Radio Science, 33, No. 3, 211-222, 1988.
[7] K. Rawer, and D. Bilitza, "International Reference Ionosphere-Plasma densities: Status 1988, Adv. Space Res., 10, 5, 1990.
[8] R. R. Vondrak, G. Smith, V.E. Hatfield, R. T. Tsunode, V. R. Frank, and P. D. Perreault, "Chatonika model of the high latitude ionosphere for applications to HF propagation predictions," Rep. 6056, RADC-TR-78-7, SRI Int., Monlo Park CA. 1978.
[9] D. N. Anderson, "A theoretical study of the ionosphere F-region equatorial anomaly, II, Results in the American and Asian sectors," Planet. Space Sci., 21, 421, 1973.
[10] R. G. Ezquer, L. Scida, G. A. Mansilla, M. Mosert, and M. F. Herrera, "F2 region maximum electron density height predictions for South America latitudes," Radio Science, Vol. 38, No. 4, pp.15-1 : 15-11, 2003.
[11] Stewart, F. G., "Ionospheric Communications Enhanced Profile Analysis & Circuit (ICEPAC) Prediction Program," Technical Manual, available for download on the Internet at http://elbert.its.bldrdoc.gov/pc_hf/hfwin32.html.
[12] G. Lane,**.** **"**Signal-to-Noise Predictions Using VOACAP, Including VOAAREA," A user's Guide. Published by Rockwell Collins (350 Collins Road NE, Cedar Rapids, IA 52498). 2001.
[13] G. Lane, and H. V. Vo., "VOACAP Method 30; A Long Path / Short Path Smoothing Function," HF Modeling & Propagation *{HFMAP} Newsletter*, Vol. 2, No. 2, 5-6, Summer-Fall 1995.
[14] D. L. Lucas, and G. W. Haydon, "Predicting Statistical Performance Indexes for High Frequency Ionospheric Telecommunications Systems," ESSA Technical Report IER 1-ITSA 1, August 1966.
[15] George Lane, "Review of the High Frequency Ionospheric Communications Enhanced Profile Analysis & Circuit (ICEPAC) Prediction Program," 2B-1, Ionospheric Effects Symposium, Alexandria VA USA, May 3-5, 2005.
[16] J. L. Lloyd, G. W. Haydon, D. L. Lucas and L. R. Teters, "Estimating the Performance of Telecommunication Systems Using the Ionospheric Transmission Channel; Volume I: Techniques for Analyzing Ionospheric Effects Upon HF Systems (DRAFT)," US Army CEEIA Tech. Rpt. EMEO-PED-79-7, 1978.
[17] A. F. Barghausen, J. W. Finney, L. L. Proctor and L. D. Schultz, "Predicting Long-Term Operational Parameters of High-Frequency Sky-Wave Telecommunication Systems," ESSA Technical Report ERL 110- ITS 78, May 1969.
[18] A. L. Barghausen, J. W. Finney, L. L. Proctor, and L. D. Shultz, "Predicting long-term operational parameters of high frequency sky-wave telecommunication systems, ESSA Tech. Rep. ERL 110-ITS 78, 1969.
[19] Lane, G., E. J. Konjicija, G. Dixon, and C. Tyson, "Efficacy of Extremely Long Distance HF Radio Broadcasts As Determined by Predictions and Measurements," Ionospheric Effects Symposium, Alexandria, VA; 3B2-1 - 3B2-7, May 4-6,1999.
[20] A. Bhattacharyya, B. Engavale, D. Tiwari and S. Bose, "Effect of solar variability on transionospheric radio wave propagation in the equatorial region," ILWS workshop 2006, GOA, February 19-24, 2006.
[21] W. F. Utlaut and R. Cohen, "Modifying the ionosphere with intense radio waves," Science, 174:245–254, 1971.
[22] A. Y. Wong and R. J. Taylor, "Parametric excitation in the ionosphere," Phys. Rev. Lett., 27(10):644–647, 1971.
[23] H. C. Carlson, W. E. Gordon, and R. L. Showen, "HF induced enhancements of incoherent scatter spectrum at Arecibo," J. Geophys. Res., 77:1242–1250, 1972.

[24] J. A. Fejer, " Ionospheric modification and parametric instabilities," Rev. Geophys. Space Phys., 17(1):135–154, 1979.
[25] V. L. Frolov, G. N. Boiko, S. A.Metelev, and E. N. Sergeev, "On the study of artificial ionospheric turbulence by means of stimulated electromagnetic emission," Radiophys. Quantum Electron. Engl. Transl., 37:593—603, 1994.
[26] K. C. Yeh and C. H. LIU, "Theory of ionospheric waves," Academic Press, London, 1972.
[27] N. Y. Bugoslavskaya, "Solar Activity and the Ionosphere for Radio Communications Specialists," Pergamon Press Ltd., New York, 1962.
[28] A. V. Streltsov, G. M. Milikh and W. Lotko, "Simulation of ULF field-aligned currents generated by HF heating of the ionosphere," Journal of Geophysical Research, Vol. 110, A04216, doi:10.1029/2004JA010629, pp. 1-11, 2005.
[29] L. M. Kagan, N. V. Bakhmet'eva, V. V. Belikovich, A. V. Tolmacheva, and M. C. Kelley, "Structure and dynamics of sporadic layers of ionization in the ionospheric E region," Radio Science, Vol. 37, No. 6, pp.18.1 – 18.12, 2002.